

## Direct Synthesis of B–C–N Single-Walled Nanotubes by Bias-Assisted Hot Filament Chemical Vapor Deposition

W. L. Wang,<sup>†</sup> X. D. Bai,<sup>†,‡</sup> K. H. Liu,<sup>†</sup> Z. Xu,<sup>†</sup> D. Golberg,<sup>§</sup> Y. Bando,<sup>§</sup> and E. G. Wang<sup>\*,†</sup>

*Beijing National Laboratory for Condensed Matter Physics, Institute of Physics, Chinese Academy of Sciences, Beijing 100080, China, International Center for Young Scientists, National Institute for Materials Science, Namiki 1-1, Tsukuba, Ibaraki 305-0044, Japan, and Advanced Materials and Nanomaterials Laboratories, National Institute for Materials Science, Namiki 1-1, Tsukuba, Ibaraki 305-0044, Japan*

Received January 29, 2006; E-mail: egwang@aphy.iphy.ac.cn

Soon after the discovery of carbon nanotubes, the ternary system of BCN nanotubes began to attract increasing research interest.<sup>1–3</sup> A prime advantage of the BCN nanotubes over their carbon counterparts is the relative simplicity in controlling the tube electronic properties.<sup>2,3</sup> A pristine carbon single-walled nanotube (C–SWNT) may behave either as metal or as semiconductor with varying band gaps, depending sensitively on the tube diameter and chirality whose control remains a formidable challenge for all known synthetic methods. By contrast, the electronic structure of BCN nanotubes is predicted to be controlled largely by their chemistry rather than their geometry, such that the band gap could be tailored over a wide range merely by varying the tube's chemical composition.<sup>2,3</sup>

Direct synthesis of the B- and N-doped multi-walled carbon nanotubes (BCN–MWNTs) was first attempted by Stéphan et al. in 1994.<sup>2a</sup> Since then, considerable progress has been made in the synthesis of the ternary BCN–MWNTs and/or nanofibers by different means of arc-discharge, laser ablation, and chemical vapor deposition (CVD).<sup>2,4,5</sup> At the same time, theoretical understanding of the structural and electronic properties concerning the BCN nanotubes has also been largely advanced.<sup>3,6</sup> The majority of the theoretical work, however, has been dealing with the SWNT structures rather than MWNTs (or nanofibers).<sup>3,6</sup> There are clearly many fundamental differences between those two systems.<sup>7</sup> Importantly, it is only the SWNTs' structure that would make the study of their intrinsic structural and physical properties easier and more valuable.<sup>3,6–8</sup> In this regard, exploring synthetic methods for producing high-quality ternary BCN–SWNTs is highly desirable, though it seems to be an even more difficult task. Up to now, the only existing example of the ternary BCN–SWNTs synthesis was achieved via an alternative post-growth treatment route, that is, by substitution reaction of the presynthesized pristine C–SWNTs with B<sub>3</sub>O<sub>2</sub> and N<sub>2</sub> at high temperature.<sup>9</sup> As far as the direct synthesis route is concerned, although a few studies showed the possibility of direct doping of C–SWNTs solely with B or N,<sup>10,11</sup> evidences for the presence of the ternary SWNTs simultaneously composed of the B, C, and N elements have not been identified yet.

Herein, we report on the direct, large-scale synthesis of ternary BCN–SWNTs via a bias-assisted hot filament CVD (HF–CVD) process. The same HF–CVD system has previously been used in our group to grow turbostratic BCN films and oriented BCN MWNTs.<sup>12</sup> This work is a continuation of our ongoing efforts toward the rational growth of BCN nanostructures. In the present contribution, the BCN–SWNTs' growth by HF–CVD was achieved

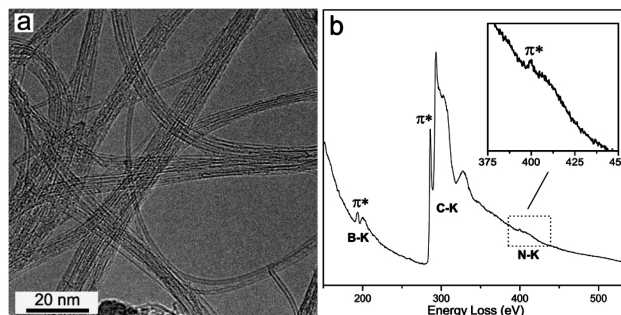


**Figure 1.** (a) TEM image of the as-grown BCN–SWNTs and (b) EELS spectrum taken from a SWNT bundle.

over the powdery MgO-supported Fe–Mo bimetallic catalyst (denoted as Fe–Mo/MgO), by using CH<sub>4</sub>, B<sub>2</sub>H<sub>6</sub>, and ethylenediamine vapor as the reactant gases. Details of the catalyst preparation and the HF–CVD growth process are presented in the Supporting Information.

In Figure 1a, we display the transmission electron microscopy (TEM) image of the as-grown BCN–SWNTs. TEM observation revealed that the as-grown SWNTs have clean and smooth surfaces with diameters in the range of 0.8–2.5 nm. Sometimes doubled-walled nanotubes (DWNTs) with slightly larger outer diameter can also be found to coexist with the SWNTs, but their amount is not dominating. An electron energy loss spectroscopy (EELS) spectrum taken from a SWNT bundle is displayed in Figure 1b, where the K-edges of B, C, and N can be clearly identified.<sup>2,4–9</sup> The sharply defined  $\pi^*$  and  $\sigma^*$  fine structure features of the C K-edge are characteristic of well-graphitized sp<sup>2</sup>-bonding carbon networks.<sup>13</sup> The B and N K-edge signals, though being much weaker, also show a discernible  $\pi^*$  peak as well as a  $\sigma^*$  band, indicating that the B and N atoms are in the same sp<sup>2</sup>-hybridized state as their C counterparts.<sup>2,4–9</sup> That is, the B and N atoms are built into the graphite network by substitutional doping, rather than gathered in the bundle intra-tube tunnels. The ternary bonding nature of the BCN–SWNTs was further confirmed by X-ray photoelectron spectroscopy (XPS) characterization (see Supporting Information, Figure S3). From the XPS spectra of B 1s and N 1s core-level electrons, the presence of sp<sup>2</sup> B–C, C–N, and B–N bonding states can be clearly identified, whereas other bonding states were not found.

For EELS elemental quantification, the detected B/C and N/C relative ratios were usually different from bundles to bundles.<sup>14</sup> We have performed numerous EELS runs on different BCN–SWNT bundles, and in most EELS runs, the N contents prevailed over those of B. The B contents usually vary in the range of 2–4 atom %, whereas the N concentration often range from 3 to 8 atom % and can, on occasion, reach as high as ~16 atom %. It is likely

<sup>†</sup> Institute of Physics, Chinese Academy of Sciences.

<sup>‡</sup> International Center for Young Scientists, National Institute for Materials Science.

<sup>§</sup> Advanced Materials and Nanomaterials Laboratories, National Institute for Materials Science.

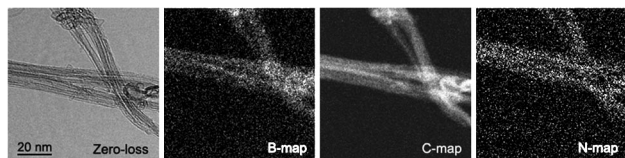


**Figure 2.** Zero-loss and energy-filtered images of two adjacent BCN-SWNT bundles.

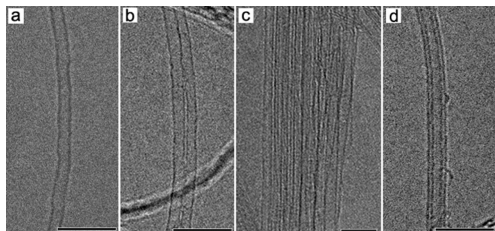


**Figure 3.** Typical HRTEM images of (a) an individual BCN-SWNT; (b) a thin SWNT bundle; (c) a thick SWNT bundle; and (d) an individual DWNT. Scale bar = 5 nm.

that the B is more difficult than N to be incorporated into the graphite lattice.<sup>10</sup>

For the as-grown BCN-SWNTs, we also succeeded in recording the energy-filtered elemental maps of B, C, and N, respectively. In Figure 2, the zero-loss and energy-filtered TEM images of two adjacent BCN-SWNT bundles are shown, where it can be seen that all constituting B, C, and N elements are homogeneously distributed within the SWNTs tube shells.

In the present study, we have conducted detailed high-resolution TEM (HRTEM) analyses of the BCN-SWNTs as well as the pristine C-SWNTs prepared via the same HF-CVD growth process. It turned out that the BCN-SWNTs are generally more deformable under the irradiating electron beam than C-SWNTs. This phenomenon is understandable when considering that the substitutional B and N atoms are localized defects within the honeycomb carbon lattice, and thus that the BCN tube shells are energetically less stable than pure carbon lattice.<sup>7,10</sup> Nevertheless, as shown in Figure 3a–d, the BCN-SWNTs normally have the straight cylindrical tube walls, a morphological feature similar to that of the pristine C-SWNTs. This is in contrast to the previously reported defective, “bamboo-like” tube structures of BCN-MWNTs,<sup>2,4,5,12</sup> but in line with the BCN-SWNTs obtained via the substitution reaction route.<sup>9</sup> Recently, the straight nonbuckled tube wall structure was also observed for the binary N-doped SWNT prepared by arc-discharge.<sup>10</sup> For the SWNT structures, it is likely that the B and/or N incorporation will introduce topological defects in the graphite shell, but not necessarily result in the defective, bamboo-like structural features.<sup>7</sup> The BCN-DWNTs coexisted with the SWNTs also exhibit similar nonbuckled hollow tube structure (Figure 3d).

Here we note that, except for SWNTs and DWNTs, the present HF-CVD growth also produced multi-walled carbon onions and a small amount of bamboo-like MWNTs. These byproducts cannot be entirely avoided, but their amount can be effectively reduced

by optimization of the growth parameters, such as the partial pressure and feeding sequence of the reactant gases, the filament temperature, the bias voltage, and growth time, etc. More importantly, optimizing the Fe–Mo/MgO catalyst is also crucial for the BCN-SWNTs growth. It is only the optimized catalyst with proper metal loading and superior textural properties that could ensure growth reproducibility and improve the selectivity toward SWNTs.

In summary, the direct synthesis of ternary BCN-SWNTs via a bias-assisted HF-CVD process was presented. The BCN-SWNTs were grown over the powdery Fe–Mo/MgO catalyst by using CH<sub>4</sub>, B<sub>2</sub>H<sub>6</sub>, and ethylenediamine vapor as the reactant gases. EELS and XPS characterization results confirmed that the B and N atoms are incorporated into the SWNTs’ lattice by substitutional doping. The element EELS mapping further indicated that all constituting B, C, and N elements are homogeneously distributed within the SWNT tube shells. HRTEM observations revealed that the as-grown BCN-SWNTs have the straight nonbuckled tube wall structure.

**Acknowledgment.** Financial support from the NSF (Nos. 10540420033, 10134030, and 10304024), MOST, and CAS of China is acknowledged.

**Supporting Information Available:** Experimental setup, methods, SEM, and XPS characterization results. This material is available free of charge via the Internet at <http://pubs.acs.org>.

## References

- Iijima, S. *Nature* **1991**, *354*, 56.
- (a) Stéphan, O.; Ajayan, P. M.; Colliex, C.; Redlich, Ph.; Lambert, J. M.; Bernier, P.; Lefin, P. *Science* **1994**, *266*, 1683. (b) Wengsieh, Z.; Cherrey, K.; Chopra, N. G.; Blase, X.; Miyamoto, Y.; Rubio, A.; Cohen, M. L.; Louie, S. G.; Zettl, A.; Gronsky, A. R. *Phys. Rev. B* **1995**, *51*, 11229. (c) Redlich, P.; Loeffler, J.; Ajayan, P. M.; Bill, J.; Aldinger, F.; Rühle, M. *Chem. Phys. Lett.* **1996**, *260*, 465.
- (a) Miyamoto, Y.; Rubio, A.; Cohen, M. L.; Louie, S. G. *Phys. Rev. B* **1994**, *50*, 4976. (b) Blasé, X.; Charlier, J.-C.; De Vita, A.; Car, R. *Appl. Phys. Lett.* **1997**, *70*, 197.
- Terrones, M.; Grobert, N.; Terrones, N. *Carbon* **2002**, *40*, 1665 and references therein.
- Ma, R.; Golberg, D.; Bando, Y.; Sasaki, T. *Philos. Trans. R. Soc. London A* **2004**, *362*, 216 and references therein.
- (a) Zhu, H. Y.; Klein, D. J.; March, N. H.; Rubio, A. *J. Phys. Chem. Solids* **1998**, *59*, 1303. (b) Lammert, P. E.; Crespi, V. H.; Rubio, A. *Phys. Rev. Lett.* **2001**, *87*, 136402. (c) Liu, Y.; Guo, H. *Phys. Rev. B* **2004**, *69*, 115401.
- Ewles, C. P.; Glerup, M. J. *Nanosci. Nanotechnol.* **2005**, *9*, 1345.
- Lee, R. S.; Gavillet, J.; de la Chapelle, M. L.; Loiseau, A.; Cochon, J.-L.; Pigache, D.; Thibault, J.; Willaime, F. *Phys. Rev. B* **2001**, *64*, 121405.
- (a) Golberg, D.; Bando, Y.; Han, W.; Kurashima, K.; Sato, T. *Chem. Phys. Lett.* **1999**, *308*, 337. (b) Golberg, D.; Bando, Y.; Bourgeois, L.; Sato, T. *Carbon* **2000**, *38*, 2017.
- Glerup, M.; Steinmetz, J.; Samaille, D.; Stéphan, O.; Enouz, S.; Loiseau, A.; Roth, S.; Bernier, P. *Chem. Phys. Lett.* **2004**, *387*, 193.
- McGuire, K.; Gothard, N.; Gai, P. L.; Dresselhaus, M. S.; Sumanasekera, G.; Rao, A. M. *Carbon* **2005**, *43*, 219.
- (a) Yu, J.; Wang, E. G. *Appl. Phys. Lett.* **1999**, *74*, 2984. (b) Bai, X. D.; Guo, J. D.; Yu, J.; Wang, E. G.; Yuan, J.; Zhou, W. *Appl. Phys. Lett.* **2000**, *76*, 2624. (c) Zhi, X. Y.; Guo, J. D.; Bai, X. D.; Wang, E. G. *J. Appl. Phys.* **2002**, *91*, 5325.
- Stéphan, O.; Sandré, E.; Ajayan, P. M.; Cyrot-Lackman, F.; Colliex, C. *Phys. Rev. B* **1996**, *53*, 13824.
- The variation of tube atomic compositions has also been observed for the BCN-SWNTs obtained via the substitution reaction, as well as the BCN-MWNTs by the direct synthesis. See, for example, refs 9 and 2b.

JA0606733